the resistances of the three zones. If we assume (1) that all wave velocities are steady, (2) that all stress amplitudes are steady, (3) that the resistivity is not time dependent, (4) that the stressed regions of the disk are in a state of one-dimensional strain, and

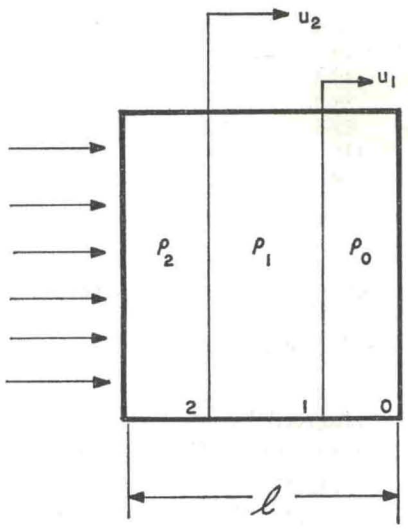

FIG. 2. Three zone resistivity model for a shock-wave loaded semiconductor. Two separate shock waves are shown as would be encountered in the stress region above the Hugoniot elastic limit.

(5) that the strains are infinitesimal;* it follows that:

$$AR(t) = \rho_0 l + U_1 t(\rho_1 - \rho_0) + U_2 t(\rho_2 - \rho_1), \qquad 0 < t < \frac{l}{U_1} \tag{1}$$

and

$$AR(t) = \rho_1 l + U_2 t(\rho_2 - \rho_1), \qquad \frac{l}{U_1} < t < \frac{l}{U_2} \tag{2}$$

where: A is the area of the disk; R is the resistance between the electrodes; ρ is the resistivity; U is the wave velocity; l is the thickness of the disk; t is the time and the subscripts 0, 1 and 2 refer to the various zones.

Equations (1) and (2) show that the electrical resistance between the electrodes of the specimen at any time is equal to the sum of the resistances of the zones. After all the waves have propagated out of the specimen without reflection, the resistance–time record will exhibit a final value corresponding to the impact stress. The initial and final values of the resistance are connected by a continuous line made up of segments of different slope, each segment corresponding to the propagation of a wavefront through the specimen. The initial and final values of the resistance explicitly define the change in resistivity due to the impact stress; the discontinuities in slope show the existence of multiple waves and define transit times for each wave from which the wave velocities can be calculated. This behavior is clearly shown in the typical record given in Fig. 3. Thus, resistance–time measurements can yield explicit data on the number of wavefronts and their wave velocities as well as the resistivity associated with each wave. Further, the complications resulting from wave reflections and subsequent interactions, which are inherent in free surface velocity techniques, are avoided.

Although it was originally hoped that values for resistivity would be obtained for the full stress range and thus provide quantitative data on the resistivities associated with the phase transition and the plastic range, experimental results show an e.m.f. for stress increments above the elastic limit which precludes quantitative resistivity measurements. Also, the temperature rise for large compressions is large and not accurately known such that resistivity is governed by the uncertain temperatures rather than the compression. The resistance–time measurements are sufficient, however, to provide good measurements of the various wave velocities, and quantitative resistivity data is obtained in the elastic range.

In order to determine the stress and specific volume, the particle velocity associated with each wave must be known in addition to the wave velocity. Because of symmetry, the total particle velocity imparted to the specimen disk is one-half the experimentally measured impact velocity.† In general the division of the total particle velocity

* It is not necessary to neglect the particle velocity (strain) to develop the analysis. It has been neglected for illustrative purposes only. All reduced data include the effects of finite particle velocity.

† The instantaneous velocity of the projectile immediately prior to impact is measured to a precision of 0·5%.[8]

Table 1. *Summary of shock wave compression data on* [111] *germanium* $\rho = 5{\cdot}35$ g/cm^3

Shot	u_p[a] (mm/μsec)	No. of waves	U_1 (mm/μsec)	U_2[b] (mm/μsec)	U_3[b] (mm/μsec)	σ_1 (kb)	σ_2[c] (kb)	σ_3[d] (kb)	$(V/V_0)_1$	$(V/V_0)_2$[e]	$(V/V_0)_3$[f]
58	0·0775	1	5·63	—	—	23·3	—	—	0·9864	—	—
59	0·1286	1	5·78	—	—	39·8	—	—	0·9778	—	—
148	0·1580	2	5·63–5·78	3·43	—	c	46·5	—	e	0·9705	—
147	0·1620	2	5·79	3·41	—	c	49·0	—	e	0·9697	—
135	0·1700	2	5·75	3·58	—	c	50·3	—	e	0·9675	—
133	0·2132	2	5·75	3·54	—	c	58·3	—	e	0·9551	—
60	0·3432	2	—	3·63	—	c	83·5	—	e	0·9193	—
149	0·5540	2	5·79	4·13	—	c	136	—	e	0·8748	—
150	0·6015	3	—	4·26	1·17	c	d	142	e	f	0·8413

[a] Particle velocity is taken as $\frac{1}{2}$ the measured impact velocity.
[b] Wave velocity relative to laboratory coordinates.
[c] Stress of the second wave is computed assuming the particle velocity of the first wave is 0·1443 mm/μsec.
[d] Stress of the third wave is computed assuming the particle velocity of the second wave is 0·5778 mm/μsec.
[e] Volume computation assumes particle velocity of first wave is 0·1443 mm/μsec.
[f] Volume computation assumes particle velocity of second wave is 0·5778 mm/μsec.

between multiple waves is unknown for a single experiment; however, if in a series of experiments the total particle velocity is systematically varied in the immediate neighborhood of a suspected cusp in the stress–volume relation until a change in the number of waves is observed, the particle velocity associated with each of the multiple waves is established. The stresses and volumes associated with any multiple wave structure can then be calculated from conservation of mass and momentum relationships,[9] if it is assumed that the particle velocity associated with a cusp is independent of driving pressure.

SECTION 2
SHOCK COMPRESSION RESULTS

Two cusps in the stress–volume relation are revealed in the data summary shown in Table 1. For a particle velocity, u_p, less than 0·1286 mm/μsec a single wave is observed and at $u_p = 0{\cdot}1580$ mm/μsec two waves are observed. Thus, a cusp exists between these two values of particle velocity. From $u_p = 0{\cdot}1580$ mm/μsec to 0·5540 mm/μsec two waves are observed, while at $u_p = 0{\cdot}6015$ mm/μsec three waves are observed.

The first of the two cusps observed and investigated is at a stress of 44 ± 4 kb which corresponds to the transition between elastic and plastic behavior, and the second is at a stress of about 140 kb which we will show is the solid–solid phase transition observed by MINOMURA and DRICKAMER[10] at a pressure of about 120 kb. Before considering the properties of the transition the shock wave compression at lower stresses must be examined.

Hugoniot elastic limit

The leading wave is identified as an elastic wave by comparison of the wave velocity with the low signal wave velocity[12] of 5·54 mm/sec. The wave velocity is somewhat higher than the low signal velocity, but this is to be expected on the basis of the finite compressions in the shock experiment. There is no detectable volume change ($< 0{\cdot}5\%$) associated with the cusp at 44 kb; thus this cusp is clearly not identifiable as a first order phase transition.

The particle velocity of the elastic wave as obtained by other investigators is shown in Table 2. There is a wide variance in values obtained by

Table 2. *Various values for the particle velocity of the elastic wave of* [111] Ge

WACKERLE[11]	MCQUEEN[13]
0·153 mm μsec^{-1}	0·114 mm μsec^{-1}
0·161 mm μsec^{-1}	0·134 mm μsec^{-1}
0·168 mm μsec^{-1}	
0·178 mm μsec^{-1}	